THE ANNALS OF "DUNĂREA DE JOS" UNIVERSITY OF GALAȚI
FASCICLE V, TECHNOLOGIES IN MACHINE BUILDING,
ISSN 1221- 4566, 2014

SIMULATION OF T TUBES HYDROFORMING

Viorel PĂUNOIU, Vasile MARINESCU, Eugen GĂVAN

Department of Manufacturing Engineering, "Dunarea de Jos" University of Galati, Romania
viorel.paunoiu@ugal.ro

ABSTRACT

Tube Hydroforming is an advanced technology used on a large scale to obtain complex parts for different applications. The paper presents the results of hydroformed T tube simulations, using FEM, in order to study the influence of radius of hydroforming die corner, cycle time and internal pressure toward the hydroformability. The axial feeding of punches remains constant and it was used to increase the tube formability. The analyses provided information about hydroformability considering the tube deformation, thickness and stress variations for the deformation conditions conducted.

KEYWORDS: tube hydroforming, hydroforming, hydroformability, FEM, simulation

1. INTRODUCTION

Tube hydroforming is an advanced technology which is largely used for obtaining different parts for different applications. The complexity of such types of parts depends on the areas where they find their applications.

The fittings are one of the major applications of tube hydraulic deformation. The most common fittings are those with three symmetrical (T tubes) or eccentric ends and elbows, which are small in dimensions and are made in general from materials with low strength. Fittings with flanges are not obtained by hydroforming. The manufacture of T fittings for plumbing from wrought-metal [21] and copper [22] tubes was the early application of this technology.

For T tubes, the hydroforming has two main advantages: the reduction of tooling costs and the elimination of welding phase, leading to the improved mechanical characteristics and superior surface quality.

In scientific literature different studies are available concerning different aspects of tube hydroforming. The basics of tube hydroforming processes as well as the industrial application of such processes are the objectives of the papers presented in [1-7, 19]. The material formability is the objective of the papers [8-11]. The optimum conditions of deformation in tube hydroforming are studied in [12-14]. FEM is largely used in studying the influence of material and process parameters on the necking and bursting in the hydroforming process [15-19].

In this work, numerical simulation has the goal to analyse the influence of process parameters: radius of hydroforming die corner, cycle time and internal pressure toward the hydroformability. A characterization of tube hydroforming is also presented.

2. PROCESS CHARACTERIZATION

The hydroforming process for a typical T tube follows the sequence illustrated in figure 1.

The tube is placed between the dies (figure 1.a). The dies are closed. Then the tube is filled with hydraulic fluid and the necessary internal pressure for deformation is provided.

Axial punches are used to seal the tube and to avoid any pressure losses (figure 1.b). After that the fluid pressure within the tube is increased with simultaneous application of the axial feeding of punches, having as a result the pushing of the material into the deformation zone (figure 1 c). The proper combination of axial feeding (F_{axial}) and internal pressure (p) assures the proper conditions for the hydroforming process evolution. A counter force could be applied toward the tube bulge. In final stage a calibration phase is applied without any axial feeding. Finally, the T tube is taken out of the die (figure 1. d).

A hydroforming system consists of: hydroforming tool, pressure system, hydraulic punching devices and clamping device. As it was presented above, the tool consists of two dies, which assure, by closing, the part shape. The pressure

system assures the internal pressure for tube deformation. The hydraulic punching devices are designed to seal the tube ends. The clamping device is used for opening and closing the two parts of the hydroforming tool.

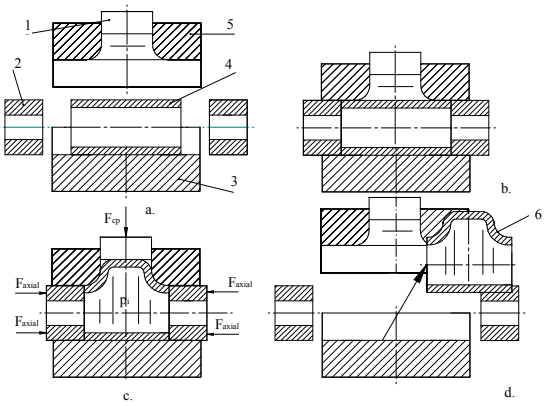

Fig. 1. *T Tube hydroforming process: 1 - counter punch; 2 - axial punches; 3 - inferior die; 4 - tube; 5- superior die; 6 - part; a. feeding; b. die closing; c. pressurization and axial feeding of punches; d. part removal*

The hydroformig process depends on the material parameters (flow curve, Poisson's ratio, strength coefficient, strain hardening exponent, anisotropy), geometry of the die and the energy parameters (fluid pressure, punch velocities, counter force and friction). The combination of the internal pressure and the axial feeding of punches is the key for a successful deformation.

3. SIMULATION MODEL

Nowadays simulation using finite element proves to be the principal method for hydroforming process investigation, in terms of strain and stress analysis, forces prediction and formability evaluation. The Dynaform with its hydroforming module is an important software tool for reducing the cost for shop floor trials and tooling and process design.

Figure 2 presents the model of the hydroforming tool used in simulation.

The tool model components and the blank are presented in table 1. For the tool components, rigid material is used, *Mat_rigid (Mat 20), according to the Dynaform software. So, the elastic deformation of the tool is assumed to be neglijable in raport with the plastic deformation of the tube.

The blank is a tube (Φ28.6x140x1mm) made of steel. The material for the tube has a "power" sort of behaviour:

$$\sigma = K \cdot \varepsilon^n \qquad (1)$$

where: K is the strength coefficient, K = 648 MPa; n – strain hardness exponent, n = 0.22.

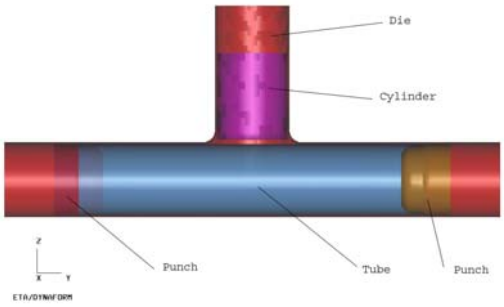

Fig. 2. *Tool model used in tube hydroforming process simulation*

The material is characterized by the following anisotropy coefficients r_{00} = 1.87; r_{45} = 1.27; r_{90} = 2.17.

In the simulated model, the tub was modelled using 3D thin shell elements with the Belytschko-Tsay element formulation, with five integration points through the thickness.

Table 1 presents the number of finite elements used for each component including the blank.

Table 1. *Tool model components*

	Active element geometry	Number of finite elements
Die corner radius R3	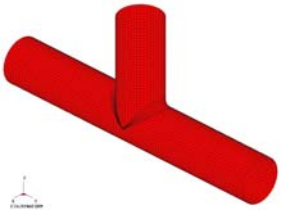	6552
Die corner radius R5		6504
Die corner radius R10		6384
Left axial punch		719
Right axial punch	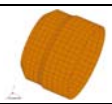	719
Counter punch (Cylinder)		435
Blank	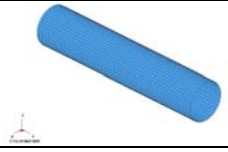	3080

In the simulation, the interfaces between the outer layer of the tube and the die, and the inner layer of the tube and inner tube integration points by thickens, which assure, by closing, the part shape punches were modelled with a contact algorithm type Contact_forming_one_way_surface_to_ surface. The friction coefficient was taken as equal to 0.1.

The pressure was applied as a surface load on the shell elements with the normal directing outward, on the inner surface of the tube, while the axial feed was applied to the punches. The two punches which simulate the hydraulic ends of the axial pistons are moving axially, with a speed of 250mm/s.

Figure 3 presents a typical curve for pressure-time variation, considering the axial moving of punches. The curve has a path of linear increasing of the pressure with the time then when the pressure is reaching the maximum value, remains constant till the end of the hydroforming process.

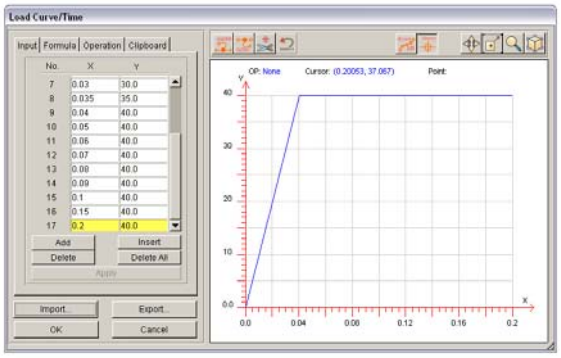

Fig. 3. *Pressure-time variation for deformation with axial moving of punches*

The counter punch acts in the simulations only with its own weight.

The analysis was done considering the following variables:

- radius of the hydroforming die corner: R3; R5 and R10.
- internal pressure, p = 10; 20; 30; 40 MPa.
- cycle time, t = 0.1s and t = 0.15s. These times provide punches displacements of 20 and 30 mm.

4. SIMULATIONS RESULTS ANALYSIS

The tube hydroforming is the result of two actions. The first action is due to the internal fluid pressure, which deforms the tube into the expansion zone of the die. Also the internal pressure determines an important friction along the die–tube interface surfaces. The second action is due to the axial feeding of the punches. The punch movement determines the material feed towards the expansion zone and facilitates the material flow even when the pressure generates a relevant friction at the die– tube interface.

The relation between the pressure and the axial feeding of punches defines the loading path.

Wrinkle occurs if the axial feed is too high with respect to the hydroforming pressure and on the contrary if the hydroforming pressure is too high with respect to the axial feed then there is a chance for the tube to burst due to excessive wall thinning.

4.1. Tube deformation

The tube deformation is explored considering the shape changing during the loading path. Some qualitative aspects of tubes deformations are presented hereunder.

Figures 4 and 5 present the shape of tubes deformations for a die corner radius R5. The cycle time is 0.1s in both cases and the axial feeding is 250mm/s. The pressure differs in figures.

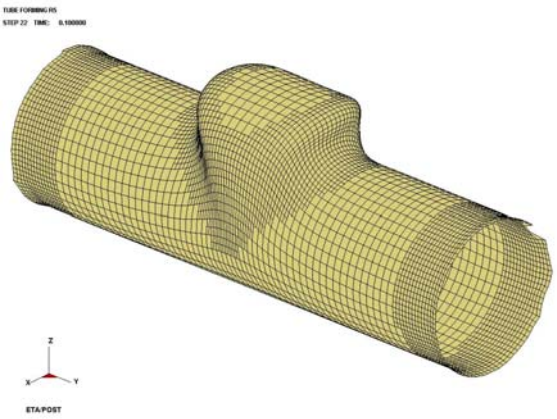

Fig. 4. *Tube deformation for a die corner radius R5, internal pressure p=10 MPa and cycle time t=0.1s*

Applying a low pressure of p=10 Mpa in the expansion zone of the die tube wrinkle occurs, figure 4. This means that there is no correlation between the axial feeding and the internal pressure. At low pressure increase, the cycle time emphasizes the improper deformation of the tube.

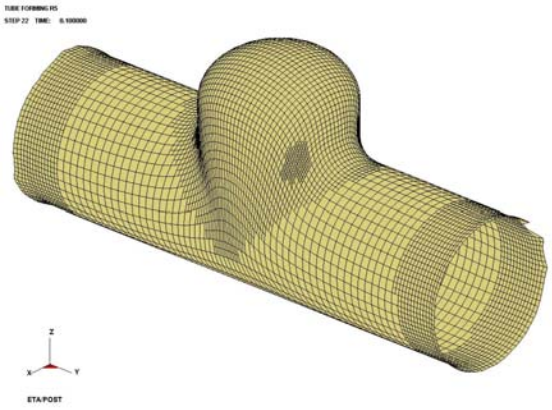

Fig. 5. *Tube deformation for a die corner radius R5, internal pressure p=40 MPa and cycle time t=0.1s*

On the other hand, increasing the pressure, in this case to 40 MPa, figure 5, the winkles disappear, and the shape of the tube in the expansion zone is appropriate.

Parts geometries obtained by hydroforming when the radius of the die is 10 mm are presented in figures 6 and 7. The cycle time is 0.15s in both cases and the axial feeding is 250mm/s. Again the pressure

differs in figures. At low pressure of p=10 Mpa, figure 6, the winkles in the expansion zone are also present.

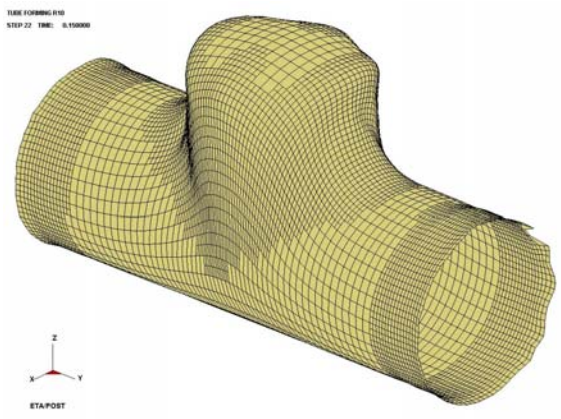

Fig. 6. *Tube deformation for a die corner radius R10, internal pressure p=10 MPa and cycle time t=0.15s*

At the pressure of 40 MPa, figure 7, the shape of the tube in the expansion zone is appropriate.

Because the cycle time is greater, the height of the tube in the expansion zone is higher.

Figures 8 and 9 present the variations of the tube bulge function of the cycle time and internal pressure.

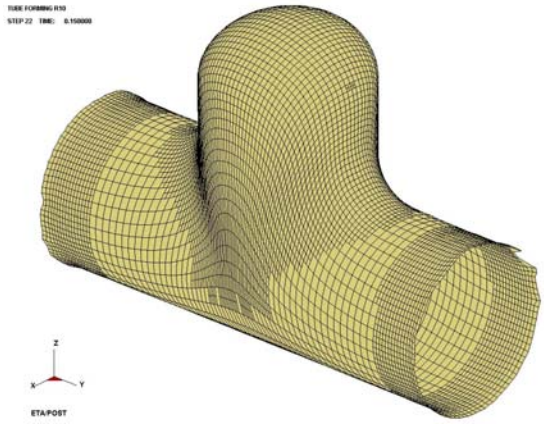

Fig. 7. *Tube deformation for a die corner radius R10, internal pressure p=40 MPa and cycle time t=0.15s*

The figures show that increasing the values of the die corner radius, the height of tube bulge will increase as well. An explanation is due to the fact that by increasing the value of the die corner radius, the friction conditions improve and the material flow in the die increases.

Increase the pressure, and the time cycle will also lead to tube bulge increase.

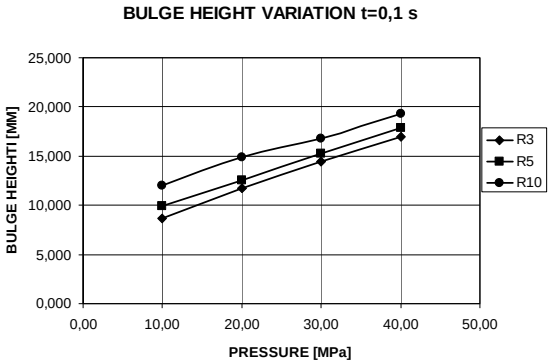

Fig. 8. *Variation of tube expansion function of corner die radius and internal pressure for a time cycle of t=0.1s*

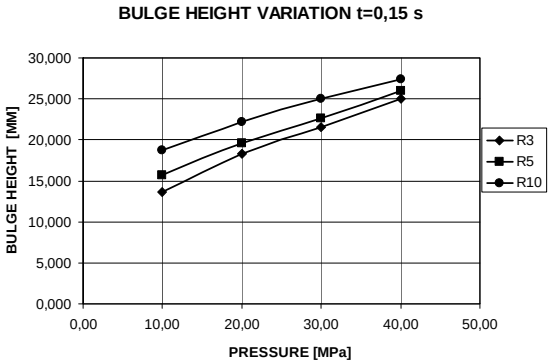

Fig. 9. *Variation of tube expansion function of corner die radius and internal pressure for a time cycle of t=0.15s*

4.2 Thickness variation

The thickness variation is an indicator of crack appearance in hydroformed tube. If material thinning is excessive, the internal pressure applied was too high. Increased axial feeding and pressure drop will result in obtaining quality parts.

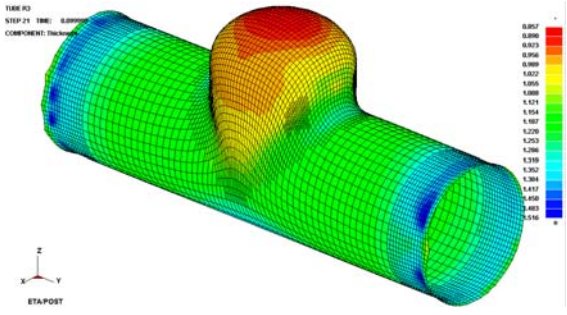

Fig. 10. *Thickness distribution for a corner die radius R3, internal pressure p=40 MPa and cycle time t=0.1s*

Figures 10 and 11 show, qualitatively, the thickness distribution of the hydroformed parts obtained for a pressure of 40 MPa and different radii.

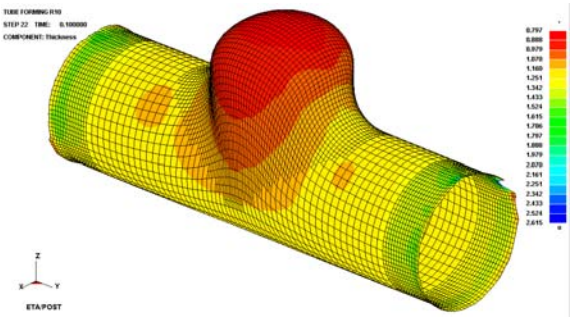

Fig. 11. *Thickness distribution for a corner die radius R10, internal pressure p=40 MPa and cycle time t=0.1s*

In all cases, the maximum thinning is localized in the protrusion area of the part. A material thickening is presented in the corner die radius. At both tube ends, the axial feeding produces a strong thickening and deformation of the material.

Table 2. *Thickness variation at the presure of 40 MPa*

		tmax, [mm]	tmin, [mm]
R3	t=0.1	1.516	0.857
	t=0.15	1.673	0.859
R5	t=0.1	2.477	0.840
	t=0.15	2.478	0.950
R10	t=0.1	2.615	0.797
	t=0.15	2.614	0.791

Table 2 presents maximum and minimum values of the material thickness, for a pressure of 40 MPa.

Increasing the corner die radius, the thickness at the protrusion area decreases, which means that the degree of thinning increases. At the same corner die radius the cycle time does not influence the degree of thinning in the protrusion area.

4.3. Von Mises stress variation

Figures 12 and 13 illustrate the variation of this tension, which is given by the relation (2):

$$\overline{\sigma} = \frac{1}{\sqrt{2}}\sqrt{(\sigma_1-\sigma_2)^2+(\sigma_2-\sigma_3)^2+(\sigma_1-\sigma_3)^2} \quad (2)$$

where σ_1, σ_2, σ_3 are the principal stresses.

The contour plots show a maximum Von Misses stress which is below the ultimate tensile strength of the blank and above the initial yield stress of the material. This confirms that the forming process occurred within the plastic region.

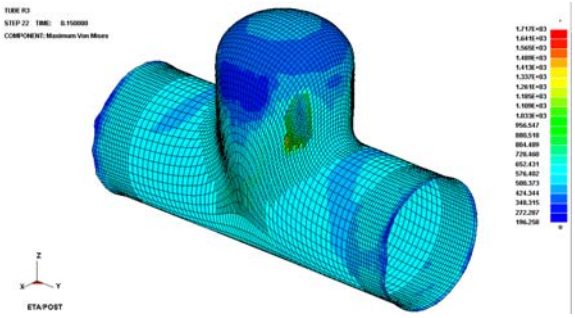

Fig. 12. *Von Mises stress distribution for a corner die radius R3, internal pressure p=40 MPa and cycle time t=0.15s*

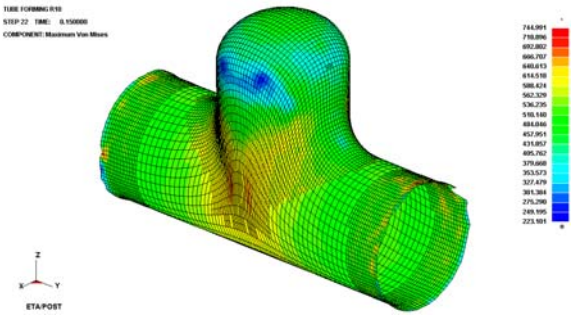

Fig. 13. *Von Mises stress distribution for a corner die radius R10, internal pressure p=40 MPa and cycle time t=0.15s*

Table 3 presents maximum and minimum values of Von Mises stress, for a presure of 40 MPa.

Table 3. *Von Mises variation at the presure of 40 MPa*

		Von Mises min, [MPa]	Von Mises max, [MPa]
R3	t=0.1	238.053	1,265e+03
	t=0.15	196.258	1,717e+03
R5	t=0.1	238.321	1.274e+03
	t=0.15	235.692	1,641e+03
R10	t=0.1	255.207	735.118
	t=0.15	223.101	744.991

Increasing the corner die radius, the maximum Von Mises stress decreases. At the same radius, the cycle time leads to an increase of maximum Von Mises values. The minimum Von Mises is almost the same in all the cases, which shows that the yielding is present at the same value which depends on the material yield point.

4.4. Mean stress variation

The mean stress is given by:

$$\sigma_{med} = \frac{\sigma_1+\sigma_2+\sigma_3}{3} \quad (3)$$

Table 4 presents values of the mean stress, for a pressure of 40 MPa. The mean stress is the negative of the pressure, p.

Table 4. *Mean stress variation at the pressure of 40 MPa*

		Mean stress, min, [MPa]	Mean stress, max, [MPa]
R3	t=0.1	-274.223	322.104
	t=0.15	-274.014	374.656
R5	t=0.1	-285.642	342.371
	t=0.15	-233.828	363.668
R10	t=0.1	-273.842	355.727
	t=0.15	-275.984	377.466

Values of mean stresses are almost the same, for all simulation cases. In the tube there are regions where values are negative, which means that the stress state is compression (linear zone of the die) and in other regions values are positive, which means stretching (zone of protrusion). There are also regions where the mean stress equals zero.

4.5. Forming Limit Diagram (FLD)

Using FLD diagrams, the failure during material deformation could be predicted. Hydrostatic pressure enhances the ductility and so it enhances the FLD.

The boundaries between safe and failed regions are represented in the forming limit diagram. The simulation shows that the tube deformation takes place in the safety zone. Deformations are charactersitic to pure shear and uniaxial compression, figure 14.

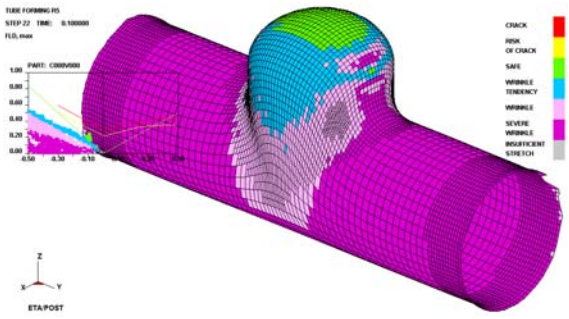

Fig. 14. *FLD distribution for a corner die radius R5, internal pressure p=40 MPa and cycle time t=0.1s*

4.6. Force variation

Figures 15 and 16 present two typical forms of the force curves when the corner die radius is R10, internal pressure p=40 MPa and cycle time t=0.15s. The following were considered: axial force on *y* direction which is given by the axial feeding of the punches and the force on *z* direction which is given by cumulative effect of the pressure and axial feeding.

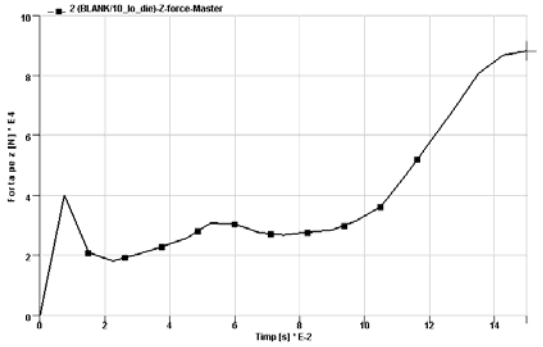

Fig. 15. *Force on z for a corner die radius R10, internal pressure p=40 MPa and cycle time t=0.15s*

While the axial force on y, figure 16, is continuously increasing, the force on z, figure 15, has three zones: one of growth, the second one almost constant and the last one of growth. The first part corresponds to the first moments of deformation, when the axial punches start to push the material in the die and the pressure is applied. The second part corresponds to axial moving of the material in the die, upon the action of the pressure and axial moving of the punches. The third one corresponds to the moment of protrusion development in the die.

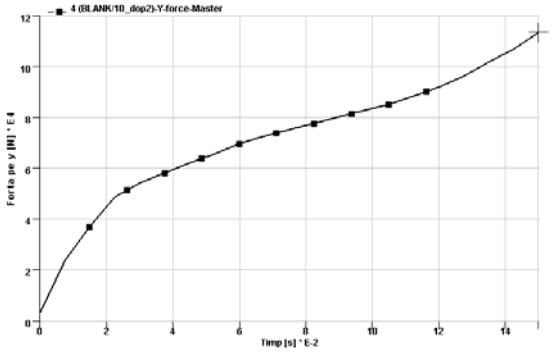

Fig. 16. *Force on y for a corner die radius R10, internal pressure p=40 MPa and cycle time t=0.15s*

Figures 17 and 18 present the variations of z force, for the considered die corner radius and pressure values.

In both cases the force decreases when the pressure increases. An explanation is due to the fact that by increasing the value of pressure, under the axial moving of the punches, the material flow in the die will increase because the friction diminishes. The increasing of the die corner radius comes also to improve the material flow in the die will increase. Increasing the cycle time leads to increasing values of *z* forces.

Figures 19 and 20 present the variations of y axial force, for the considered die corner radius and pressure values.

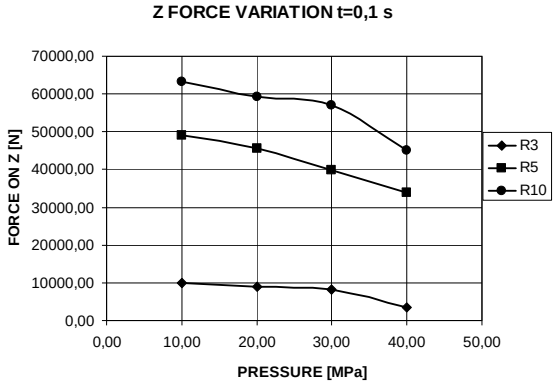

Fig. 17. *Z force variation, cycle time t=0.1 s*

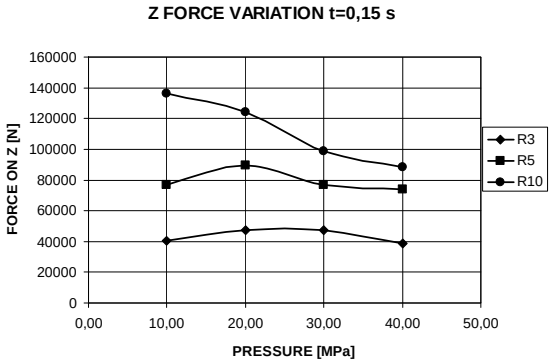

Fig. 18. *Z force variation, cycle time t=0.15 s*

In both cases the force also decreases when the pressure and corner die radius increases. The decrease is much smaller in comparison with *z* force. Increasing the cycle time leads to increasing values of y axial forces.

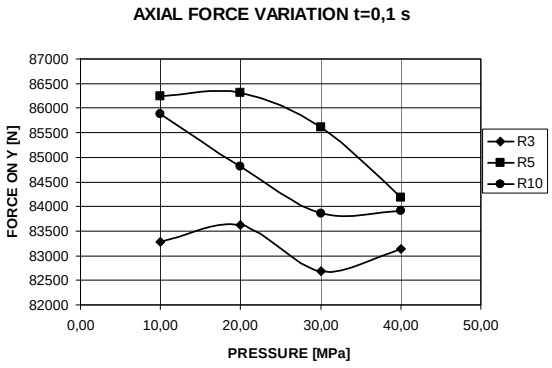

Fig. 19. *Axial force y, cycle time t=0.1 s*

5. CONCLUSIONS

The paper presents initially a bibliographical study of tube hydroforming technology, about the effects of the forming parameters on the quality of the part.

Then, a process characterisation of T tube hydroforming is illustrated. Next, using the software Dynaform, the methodology for building the simulation model of T tube hydroforming is presented.

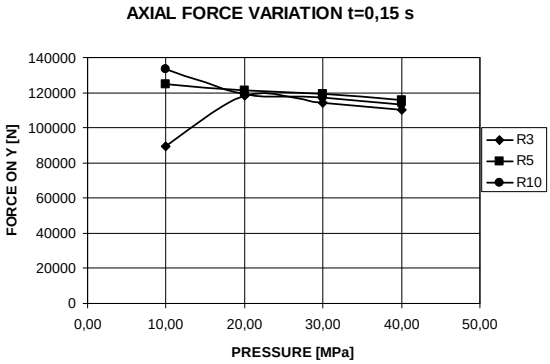

Fig. 20. *Axial force y, cycle time t=0.15 s*

A total of 24 simulations of a T tube hydroforming were made. In these simulations a number of parameters changed, namely: the radius mold, work pressure, cycle time. The results show:

- at small pressure the parts are wrinkled, especially in the protuberance zone. This shows that there is no correlation between the axial feeding of the punches, that is great, and the pressure, that is small. Increasing cycle time, at low pressure, increases improper deformation of the workpiece;
- by increasing the corner die radius, the pressure at which corresponding parts decreases are obtained;
- by increasing the corner die radius, the T bulge height will increase;
- by increasing the pressure and the cycle time the T bulge height will increase;
- the maximum thinning is obtained in the maximum zone of the protrusion. A material thickening appears at the corner die radius. At both ends the material is thicker because of the pressure exercised by punches;
- the deformation occurs in the safety zone regardless of the corner die radius and cycle time;
- forming limit curve shows that in all cases there is no risk of rupture in the material;
- for the axial feeding considered, the minimum pressure at which it can discuss about a sound product is 30 MPa;
- by increasing the corner die radius, the value of the *z* force decreases with the pressure increase, at the same axial feeding of the punches, and in the same time it decreases with die corner radius, at the same pressure. Increasing the corner die radius and pressure does not greatly affect the value of the axial force. It increases with increasing cycle time.

REFERENCES

[1] Sokolowski, T., Gerke, K., Ahmetoglu, M., Altan, T., *Evaluation of tube formability and material characteristics: hydraulic bulge testing of tubes*. J. Mater. Processing Technol., 2000, 98, 34–40;

[2] Ahmetoglu, M., Altan, T., *Tube hydroforming: state-of-the-art and future trends*. J. Mater. Processing Technol., 2000, 98, 25–33;

[3] Dohmann, F., Hartl, Ch., *Tube hydroforming: research and practical application*, J. Mater. Processing Technol., 1997, 71, 174–186;

[4] Dohmann, F., Hartl, Ch., *Hydroforming–a method to manufacture light-weight parts*, J. Mater. Processing Technol., 1996, 60, 669–676;

[5] Koc, M., Altan, T., *An overall review of the tube hydroforming (THF) technology*, J. Mater. Processing Technol., 108, 384-393, 2001;

[6] Liewald, M., Pop, R., Wagner, S., *Magnesium Tube Hydroforming, 10th ESAFORM Conference on Material Forming*, 2007, American Institute of Physics 978-0-7354-0414-4;

[7] Asnafi, N., *Analytical modeling of tube hydroforming*, Thin-walled structures, 34, 295-330, 1999;

[8] Jeong Kim, Sang-Woo Kim Hoon, Jae Park, Beom-Soo Kang, *A prediction of bursting failure in tube hydroforming process based on plastic instability*, Int. J. Adv. Manuf. Technol. (2006) 27:518–5242;

[9] Koc, M., Altan, T., *Prediction of forming limits and parameters in the tube hydroforming process*, Int. J. Mach. Tool Manuf., 2002;

[10] Vollertsen, F., Plancak, M., *On possibilities for the determination of the coefficient of friction in hydroforming of tubes*, J. Mater. Processing Technol., 2002;

[11] Jirathearanat, S., Strano, M., Altan, T., *Selection of tube hydroforming loading paths by adaptive simulation*, Engineering Research Center for Net Shape Manufacturing, The Ohio State University, 2002;

[12] Rimkus, W., Bauer, H., Mihsein, M.J.A., *Design of load-curves for hydroforming applications*, J. Mater. Processing Technol., 108, 97-105, 2000;

[13] Labergere, C., Gelin, J.C., *New strategies for optimal control of command laws for tube hydroforming processes*, 8th ICTP Conference Proceedings, 2005;

[14] Adebrabbo, N., Worswick, M. at al., *Optimization methods for the tube hydroforming process applied to advanced high-strength steels with experimental certification*, J. Mater. Processing Technol., Vol. 209, 2009, pp. 110–123;

[15] Yang, B., Zhang, W.G., Li, S.H., *Analysis and finite element simulation of the tube bulge hydroforming process*, Int. J. Adv. Manuf. Technol. (2006)29:453–458;

[16] Nickhare, C., Weiss, M., Hodgson, P.D., *FEA comparison of high and low pressure tube hydroforming of TRIP steel*, Computational Materials Science, Vol. 47, 2008, pp. 146–152.

[17] Hama, T., Asakawa, M., Fuchizawa, S., Makinouchi, A., *Analysis of Hydrostatic Tube Bulging with Cylindrical Die Using Static Explicit FEM*, Mater. Trans., 44-5 (2003), 940-945;

[18] Hama, T., Asakawa, M., Takamura, M., Makinouchi, A., Teodosiu, C., *A Stable and Fast New Contact Search Algorithm for FEM Simulation of Metal Forming Process*, Proc. M&P2002, Hawaii, (2002), 367-372;

[19] Strano, M., Jirathearanat, S. and Altan, T., *Adaptive FEM simulation for tube hydroforming: a geometry based approach for wrinkle detection*. Ann. CIRP, 2001, 50, 185–190.

[20] *,** *Metal Forming Handbook* / Schuler (c) Springer-Verlag Berlin Heidelberg, 1998.

[21] Gray, J.E., *Apparatus for making wrought metal Ts*. U.S. Patent 2,203,868, 1940

[22] Ogura, T., Ueda T. (1968), *Liquid bulge forming*, Metalworking Prod. **24,** 4, 73–81, 1968